Local density of states from constant-current tunneling spectra

M. Ziegler, N. Néel, A. Sperl, J. Kröger,* and R. Berndt
Institut für Experimentelle und Angewandte Physik, Christian-Albrechts-Universität zu Kiel, D-24098 Kiel, Germany
(Received 30 April 2009; revised manuscript received 4 July 2009; published 4 September 2009)

Scanning tunneling spectroscopy of the differential conductance is performed at constant current and at constant distance. These modes of operation significantly affect peak positions and line shapes in spectra as well as patterns in spatial maps of the differential conductance. A normalization procedure for constant-current data, which relies on experimental current-distance data, is shown to yield spectral information on the local density of states.

DOI: 10.1103/PhysRevB.80.125402 PACS number(s): 68.37.Ef, 68.47.De, 73.20.At

I. INTRODUCTION

Tunneling experiments have been used since the work of Giaever[1] to investigate the density of electronic states. With the advent of scanning tunneling microscopy (STM),[2] tunneling data can be resolved with atomic lateral resolution and various spectroscopic modes of measurement have been developed to take full advantage of its capabilities. Methods to analyze these data have been developed and take into account the full three-dimensional character of the tunnel barrier. However, in many cases the one-dimensional Wenzel-Kramers-Brillouin tunneling theory, where the current is represented by a simple convolution of the density of states of the tip and of the sample using a tunneling matrix element, is sufficient to describe the data. While three-dimensional tunneling theories do not lead to such an expression for the current,[3] numerical results for tunneling between alkali atoms on jellium electrodes lent some justification to the simple one-dimensional approximation, which was suggested for STM by Selloni *et al.*[4] It has since been used by many authors to evaluate spectra of the differential conductance, dI/dV (I and V denote tunneling current and voltage, respectively).

As dI/dV spectra do not directly reflect the spectral local density of states (LDOS), Stroscio *et al.*[5] suggested a normalization procedure where the differential conductance is divided by the conductance. The normalized spectrum of $(dI/dV)/(I/V)$ was proposed to be similar to the surface LDOS. Calculations by Lang[6] for alkali atoms on jellium with their broad LDOS features confirmed this proposal. Ukraintsev[7] presented a comparison of various normalization schemes and proposed a normalization, which relies on a tunneling probability function fitted to the spectra. Koslowski *et al.*[8] and later Passoni *et al.*[9] suggested a normalization, which requires additional experimental input data, and yields, in the case of noise-free model data, a rather precise approximation of the LDOS. A normalization algorithm for spectroscopic data obtained from organic layers on surfaces has been proposed by Wagner *et al.*[10]

The above normalization schemes are particularly useful in evaluating dI/dV spectra, which are recorded at a constant tip–sample distance.[5] However, it can be advantageous to record spectra at constant current, which implies varying distances. For instance, covering a wide range of voltages in a single spectrum is possible, whereas it would require an extreme dynamic range of current when measuring at constant tip-sample distance. Excessive currents during spectroscopy often damage or alter molecules at surfaces. This may be avoided by spectroscopy at constant (and low) current. Moreover, mapping of dI/dV simultaneously with recording of a constant-current topograph can be performed conveniently. Similar maps at constant distance are sometimes difficult to achieve when the investigated surface exhibits prominent topographic features. Indeed, a number of recent publications reported constant-current spectra which were analyzed assuming that constant-current dI/dV spectra reflect the density of states.[11–13] So far, no modeling has been reported to evaluate the validity or precision of this assumption.

The purpose of this article is to fill this gap to some extent. Using the results of Kosloswki *et al.*,[8] dI/dV spectra at constant current are modeled and a scheme is proposed to extract the LDOS from experimental constant-current data. The scheme is tested for characteristic LDOS features such as peaks or steplike onsets. Moreover, we extend prior work by Li *et al.*,[14] who presented a procedure to obtain maps of the LDOS from constant-current dI/dV maps. The analysis schemes are used to process experimental constant-current data from C_{60} molecules and from Ag_2 clusters and the results are compared to constant-distance data. Not unexpectedly, the influence of the varying tip-sample distance on constant-current data is significant and should be taken into account if one is striving for a semiquantitative data analysis.

II. EXPERIMENT

Experiments were performed using a custom-built scanning tunneling microscope operated at 7 K and in ultrahigh vacuum with a base pressure of 10^{-9} Pa. Sample surfaces as well as chemically etched tungsten tips were cleaned by argon ion bombardment and annealing. Fullerene molecules (C_{60}) were adsorbed onto cold Au(111) surfaces using an electron beam evaporator, while Ag atoms were deposited on Ag(111) by controlled tip-surface contacts.[15] Spectra of dI/dV were recorded using lock-in detection with root-mean-square modulation amplitudes of 1–15 mV, a frequency of 10 kHz and applying the voltage to the sample. The modulation frequency exceeded the response frequency of the feedback loop to avoid modulation of the tip-sample distance in constant-current dI/dV spectroscopy. Experiments were per-

formed with many tips in order to identify and avoid tip effects.

III. MODEL

The starting point of our normalization scheme for constant-current spectra is the one-dimensional model of the tunnel barrier introduced by Simmons.[16] For low temperatures, i.e., $T \ll eV/k_B$ (k_B: Boltzmann's constant; $-e$: electron charge), the tunneling current at a tip-sample distance z and a bias voltage V is expressed as

$$I(z,V) \propto \int_0^{eV} \varrho_s(E)\varrho_t(E-eV)\mathcal{T}(z,V,E)dE, \tag{1}$$

where ϱ_s and ϱ_t are the local densities of states of, respectively, the sample and the tip, and E denotes the energy of states participating in the tunneling process. The transmission factor, $\mathcal{T}(z,V,E)$, for a trapezoidal tunnel barrier is estimated in the Wentzel-Kramers-Brillouin approximation[17,18] according to

$$\mathcal{T}(z,V,E) \propto \exp\left(-\alpha z\sqrt{\phi + \frac{eV}{2} - E}\right) \tag{2}$$

with $\alpha = 2\sqrt{2m}/\hbar$ (m: free electron mass; $\hbar$: Planck's constant divided by 2π) and ϕ the apparent tunnel barrier height. In the following, a constant tip density of states is assumed. The differential conductance at constant distance then reads ($z = z_0 = \text{const}$)

$$\frac{dI(z_0,V)}{dV} \propto e\varrho_s(eV)\mathcal{T}(z_0,V,eV) + \int_0^{eV} \frac{\partial\mathcal{T}(z_0,V,E)}{\partial V}\varrho_s(E)dE. \tag{3}$$

Following Ref. 8 the second term in Eq. (3) (which may become significant for elevated voltages, but is often neglected) is approximated leading to

$$\frac{dI(z_0,V)}{dV} \propto e\varrho_s(eV)\mathcal{T}(z_0,V,eV) - \frac{e\alpha z_0}{\sqrt{\phi}}I(V). \tag{4}$$

Solving Eq. (4) for ϱ_s, the LDOS is obtained from constant-distance spectra.

We now allow for a variation of the tip-sample distance, $z(V)$. The derivative of the current with respect to the voltage reads as

$$\begin{aligned}\frac{dI[z(V),V]}{dV} \propto\ & e\varrho_s(eV)\mathcal{T}[z(V),V,eV] \\ & + \int_0^{eV} \frac{\partial\mathcal{T}[z(V),V,E]}{\partial V}\varrho_s(E)dE \\ & + \int_0^{eV} \frac{dz(V)}{dV}\frac{\partial\mathcal{T}[z(V),V,E]}{\partial z}\varrho_s(E)dE.\end{aligned} \tag{5}$$

The third term, which contains dz/dV, can be discarded since for each voltage dI/dV is measured at a given distance, i.e., $dz/dV = 0$. Solving then Eq. (5) for ϱ_s using the approximations introduced in Ref. 8 leads to

$$\varrho_s(eV) = \frac{1}{e\mathcal{T}[z(V),V,eV]}\left\{\frac{dI[z(V),V]}{dV} + \frac{e\alpha z(V)}{\sqrt{\phi}}I_0\right\}, \tag{6}$$

where I_0 is the constant current set for the measurements. Equation (6) suggests that the LDOS can be determined from constant-current spectra if $z(V)$ is available. While the absolute distance, $z(V)$, is not known in experiments, measuring a tip excursion, $\Delta z(V)$, is simple and can be done simultaneously with recording $dI(V)/dV$. As will be shown below a reference distance z_0 may be estimated to obtain $z = z_0 + \Delta z$.

To test the validity of this simple approach, we applied Eq. (6) to experimental constant-current dI/dV data and compared to results from constant-distance spectroscopy. Moreover, we used typical model densities of states to numerically compare both spectroscopy modes. To simulate constant-current dI/dV spectra and the displacement of the tip [$\Delta z(V)$ curves], z was varied for a given V until the calculated current $I(z,V)$ deviated from a set, constant value I_0 by less than 0.1%.

In the cases presented below, the normalization is useful in analyzing constant-current data despite the significant approximations of the model. However, the scheme is likely to fail when the energy of the tunneling electrons approaches the apparent barrier height. Further, the electronic structure of the tip is assumed to be featureless.

IV. RESULTS AND DISCUSSION

A. Peak-shaped spectroscopic features

For a first test, experimental spectra of C_{60} molecules adsorbed on Au(111) are used [Fig. 1(a)]. The lowest and second-to-lowest unoccupied molecular orbitals (LUMO, LUMO+1) give rise to peaks in constant-current (gray line) as well as in constant-distance (black line) dI/dV spectra.[19] Compared to the constant-distance data, the constant-current peaks are shifted by ≈ 110 mV and ≈ 70 mV toward lower voltages. In addition, the relative amplitudes of the LUMO and LUMO+1 peaks are drastically different in the two spectroscopy modes.

At the low currents used for these measurements, these differences cannot be explained by the influence of the electric field between tip and sample.[20,21] Rather, they are due to the varying tip-sample distance at constant current, which is shown as a light gray line in Fig. 1(a). This can be demonstrated as follows. Using experimental constant-distance $I(V)$ and $dI(V)/dV$ data, the sample LDOS, ϱ_s, was extracted using Eq. (4) and then fitted by a superposition of two Gauss-Lorentz lines. This LDOS was implemented into Eq. (1), which was further numerically differentiated to give the calculated constant-distance dI/dV spectrum. The result of this procedure is shown in Fig. 1(b) as a black line. This optimized model LDOS was used to calculate a constant-current spectrum [gray line in Fig. 1(b)] via Eq. (1) and its numerical derivative. Figure 1(b) also shows the calculated tip displacement at constant current, $\Delta z(V) = z(V) - z_0$, as a light gray line. The calculated curves reproduce the experimentally observed energy shifts and line shapes of the orbital-related spectroscopic signatures. The differences between the constant-current and constant-distance data can therefore be

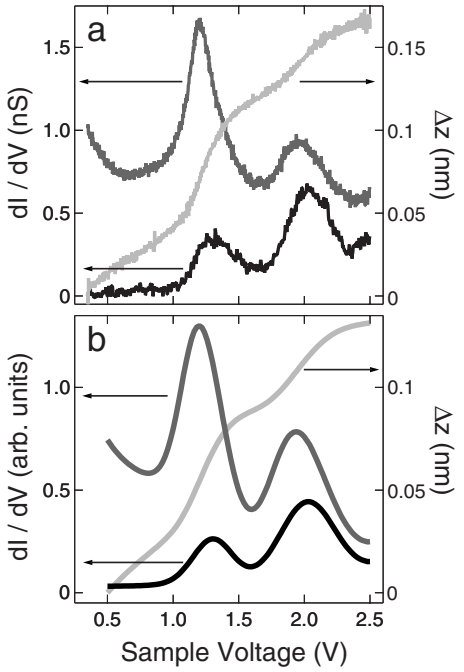

FIG. 1. (a) Experimental constant-distance (black) and constant-current (dark gray) dI/dV spectra together with displacement curve $\Delta z(V)$ (light gray) atop a single C_{60} molecule on Au(111). The tunnel gap for constant-distance spectroscopy was set at 2.5 V and 1 nA, while 1 nA was used for the constant-current spectrum. (b) Calculated constant-distance (black) and constant-current (dark gray) dI/dV spectra and $\Delta z(V)$ (light gray). For the calculations an initial tip-sample distance of 0.6 nm was used. The apparent barrier height ϕ=7.8 eV was determined from experimental current-versus-distance data.

attributed to the displacement of the tip in the course of data acquisition, as expected. By performing similar simulations for a number of peak shapes and amplitudes, some simple rules were determined: (i) increasing the width of a single peak leads to a larger shift between the corresponding peaks in constant-current and constant-distance spectra; (ii) an energy-independent background LDOS decreases the shift between these peaks; and (iii) two identical LDOS peaks give rise to different peak heights in constant-current spectra. The closer the peaks are, the more will the high-energy peak be attenuated.

Figure 2 shows a comparison of ϱ_s extracted from constant-distance (dots) and constant-current (lines) spectra, using Eqs. (4) and (6), respectively. Obviously, both methods lead to similar results. The constant-current data have been treated using three estimates of z_0, extending over a fairly wide range from 0.6 to 1 nm. According to Fig. 2 this parameter does not drastically affect the spectral shape. In particular, z_0 affects the heights of the peaks, whereas the peak positions remain almost unchanged. Taking into account only the first term of Eq. (6) leads to deviations of the extracted local density of states from the other curves in the low-voltage region (dashed line in Fig. 2, 0.5–1 V). The second term in Eq. (6) plays an important role for voltages, where a considerable change of the tip-sample distance occurs. In this case, it is not sufficient to divide constant-current dI/dV data by the transmission factor only.

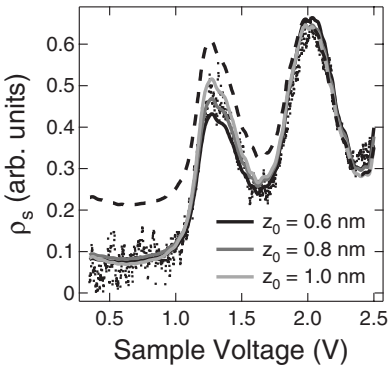

FIG. 2. Local density of states of a C_{60} molecule on Au(111) extracted from dI/dV spectra at constant distance (dots) using Eq. (4) and at constant current for the indicated initial tip-sample distances (solid lines) using Eq. (6). The dashed line shows the result of dividing constant-current dI/dV data only by the transmission factor [Eq. (6) without second term, z_0=0.8 nm, see also Ref. 14]. An apparent barrier height ϕ=7.8 eV was used for the normalization.

B. Step-shaped spectroscopic features

Step-shaped features of the LDOS are often observed from the band edges of electronic surface states, which represent quasi-two-dimensional electron gases. Occupied and unoccupied states lead to different line shapes in constant-current spectra, which will be analyzed below.

Occupied surface states occur, e.g., on the (111) surfaces of noble metals. Figure 3(a) displays constant-distance (black) and constant-current (gray) spectra of Cu(111) along with the tip displacement curve (light gray) acquired simul-

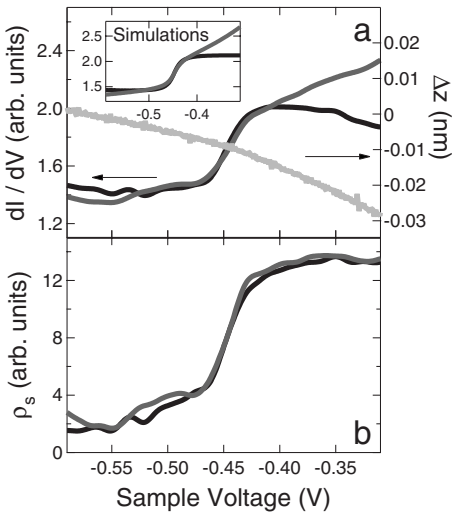

FIG. 3. (a) Constant-distance (black) and constant-current (gray) spectra of dI/dV of the occupied Cu(111) surface state along with the tip displacement curve (light gray), Δz. The feedback parameters prior to spectroscopy were set to −0.6 V and 1 nA. Inset: simulation of constant-distance and constant-current spectra for a sample LDOS according to Eq. (7) with parameters E_0 =−445 meV, Γ=24 meV, ϕ=4 eV, and z_0=0.5 nm. (b) Extracted sample LDOS, ϱ_s, from constant-distance and constant-current spectra shown in (a) using Eqs. (4) and (6).

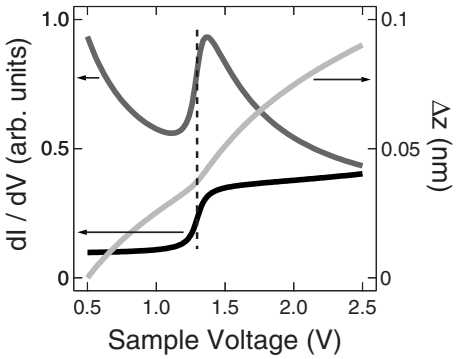

FIG. 4. Calculated constant-distance (black) and constant-current (gray) spectrum together with tip displacement characteristics (light gray) for a model LDOS of an unoccupied surface state [Eq. (7)]. The dashed line indicates the middle of the step-like onset (E_0=1.35 eV), which coincides with the inflection point of the displacement curve.

taneously with the constant-current spectrum. The band edge of this state is located ≈−445 meV below the Fermi level and causes the rapid change of the conductance at the corresponding sample voltage. While the constant-distance spectrum is rather flat above this onset, the constant-current signal keeps increasing.

For modeling, the density of states of a two-dimensional electron gas with finite lifetime was used[22]

$$\varrho_s(E) = \frac{1}{2} + \frac{1}{\pi}\arctan\left[\frac{2(E-E_0)}{\Gamma}\right] + \varrho_b. \qquad (7)$$

E_0 is the energy of the band edge, Γ is proportional to an inverse lifetime and controls the width of the onset,[22] ϱ_b denotes the background LDOS of bulk electronic structure, which is assumed to be constant over the narrow relevant energy range. Calculated spectra are shown in the inset to Fig. 3(a) and reproduce the experimental trend.

Figure 3(b) compares the LDOS extracted directly using Eqs. (4) and (6) from the experimental constant-distance spectrum (black) and from the constant-current spectrum (gray). The results show the expected steplike onset and are in good agreement.

For completeness, we also include modeling results for an unoccupied surface state. Figure 4 shows calculated constant-current and constant-distance spectra based on a sample LDOS given by Eq. (7) with E_0=1.35 eV and Γ =0.1 eV. These parameters approximately mimick the unoccupied surface state of Pd(111) as measured by time-resolved two-photon photoemission.[23] The deviations between the constant-distance dI/dV spectrum (black) and the constant-current dI/dV data (gray) are rather drastic and may be understood by the displacement curve (light gray). As the voltage is increased over the band edge, the tip is rapidly retracted to keep the current constant. As a consequence, the transmission $\mathcal{T}$ is reduced and dI/dV decreases. The different appearance of the occupied surface state in Fig. 3 is consistent with this interpretation. As the bias is varied from −0.6 to −0.3 V, the tip approaches the surface. This leads to an increase of $\mathcal{T}$ explaining the observed increase of constant-current dI/dV data in this energy range.

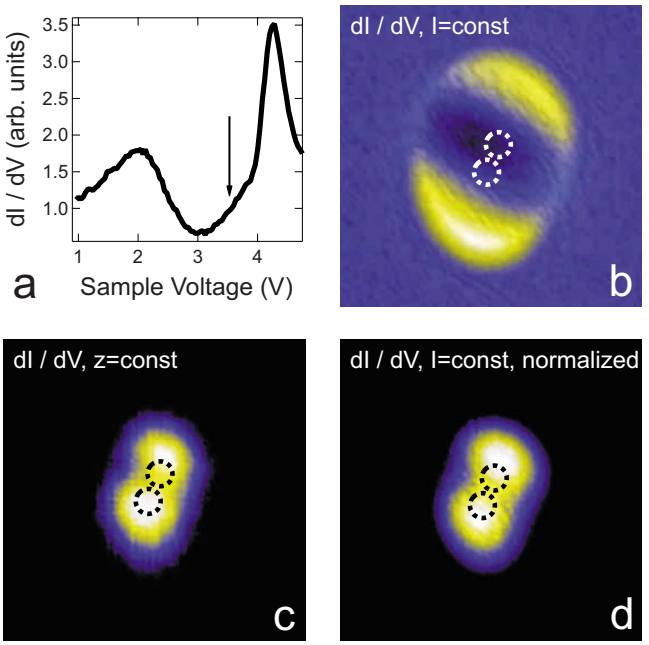

FIG. 5. (Color online) (a) Constant-current (1 nA) spectrum of dI/dV acquired at the center of a Ag dimer adsorbed on Ag(111). The arrow marks the voltage, at which maps of dI/dV are taken. (b) Constant-current and (c) constant-distance map of dI/dV recorded at 3.5 V, 1 nA over a 3 nm×3 nm area. Dashed circles indicate the positions of the dimer atoms. (d) Spatial map of normalized constant-current dI/dV for the Ag dimer shown in (b) and (c), which was extracted by using Eq. (6) for each image point. An apparent barrier height ϕ=5 eV and a tip-sample distance z_0 =0.5 nm were used for the simulations.

C. Maps of the differential conductance

Constant-current mapping of dI/dV (or I) has been discussed by Stroscio *et al.*[24,25] and by Berghaus *et al.*[26] Topographic features lead to significant variations of the dI/dV signal and complicate the interpretation of the data. In the context of surface state scattering on flat Ag(111) surfaces, Li *et al.*[14] dealt with this problem by normalizing dI/dV data using a transmission factor according to the first part of Eq. (6). Below, we apply the normalization procedure [entire Eq. (6)] to an illustrative example of a more corrugated structure, namely a Ag dimer (Ag_2) adsorbed on Ag(111).

In constant-distance dI/dV spectra Ag_2 exhibits a sp_z resonance at ≈2.4 V,[27,28] which shifts to ≈2 V in constant-current spectra [Fig. 5(a)]. Beyond ≈3 V the dI/dV signal increases owing to a field-emission resonance.[29,30] Within the rise a shoulder around 3.5 V [arrow in Fig. 5(a)] is observed, which may be assigned to an antibonding resonance of the dimer.[28] A constant-current map of dI/dV acquired at 3.5 V is shown in Fig. 5(b). Sickle-shaped maxima are visible at both ends of the dimer, which is oriented along a close-packed direction of the host lattice [dashed circles in Fig. 5(b) indicate the positions of the Ag atoms of the dimer]. A constant-distance map of dI/dV acquired on the dimer at the

same voltage is presented in Fig. 5(c). Most obviously, the spatial extension of the dimer signal is strongly reduced compared to the constant-current dI/dV map. The centers of the circularly shaped maxima of the dI/dV map are $\approx$0.43 nm apart while for the constant-current dI/dV map a distance of $\approx$1.46 nm is found. Simulations of constant-current and constant-distance dI/dV cross-sectional profiles through the dimer along the close-packed Ag(111) direction reproduced these observations.[31] The comparison between constant-current [Fig. 5(b)], constant-distance [Fig. 5(c)] and normalized constant-current dI/dV [Fig. 5(d)] maps demonstrates that constant-distance maps of dI/dV are more closely related to the sample LDOS, as has been suggested previously.[32] The peculiar pattern in the constant-current dI/dV map of the dimer arises from the presence of antibonding states at the edges of the dimer and their absence from its center. For a voltage corresponding to the antibonding state energy, the increase of the LDOS at the dimer edges gives rise to high constant-current dI/dV signals at these positions. At the center of the dimer the antibonding state is absent, while the bonding state with an appreciably different energy of $\approx$2 eV [Fig. 5(a) and Ref. 28] is present. As a consequence, the constant-current dI/dV signal is even lower than on the Ag(111) surface.[24]

Our normalization procedure also works for structures with low corrugations such as LDOS oscillations resulting from surface state scattering at step edges[14,33] and from confinement to nanostructures.[34–37] A word of caution is necessary concerning a possible variation of the apparent barrier height, which enters as a constant in Eq. (6). The apparent barrier height may be modified by changes of the work function, which are significant for, e.g., alkali metal atoms adsorbed on metal surfaces.[38–40] Lateral variations of the apparent barrier height may also be induced by modifications of the tip-sample distance and by a changing ratio of tip and sample LDOS.[8] Comparing current-distance curves acquired at low voltages on bare Ag(111) and on Ag_2 we found that apparent barrier heights differ by $\approx$0.5 eV, which represents a rather small change and does not influence the presented results significantly.

V. CONCLUSION

Spectra of dI/dV at constant current can be used to obtain information about the LDOS of structures at surfaces. The excursion of the tip during constant-current data acquisition leads to significant deviations compared to constant-distance data. We propose a simple normalization scheme, which takes into account experimental current-distance characteristics. For a number of density of states features, which are often observed in experiments, the normalization yields a quantity which is close to the LDOS.

ACKNOWLEDGMENTS

We thank A. Franke and E. Pehlke (University of Kiel) for discussions and for providing unpublished calculations. Financial support by the Deutsche Forschungsgemeinschaft (SFB 668 and SFB 677) and by the Innovationsstiftung Schleswig-Holstein is gratefully acknowledged.

*kroeger@physik.uni-kiel.de

[1] I. Giaever, Phys. Rev. Lett. **5**, 147 (1960); **5**, 464 (1960).
[2] G. Binnig, H. Rohrer, Ch. Gerber, and E. Weibel, Appl. Phys. Lett. **40**, 178 (1982); Phys. Rev. Lett. **49**, 57 (1982); Physica B & C **109-110**, 2075 (1982); G. Binnig and H. Rohrer, Helv. Phys. Acta **55**, 726 (1982).
[3] J. Tersoff and D. R. Hamann, Phys. Rev. Lett. **50**, 1998 (1983); Phys. Rev. B **31**, 805 (1985).
[4] A. Selloni, P. Carnevali, E. Tosatti, and C. D. Chen, Phys. Rev. B **31**, 2602 (1985).
[5] J. A. Stroscio, R. M. Feenstra, and A. P. Fein, Phys. Rev. Lett. **57**, 2579 (1986).
[6] N. D. Lang, Phys. Rev. B **34**, 5947 (1986).
[7] V. A. Ukraintsev, Phys. Rev. B **53**, 11176 (1996).
[8] B. Koslowski, C. Dietrich, A. Tschetschetkin, and P. Ziemann, Phys. Rev. B **75**, 035421 (2007).
[9] M. Passoni, F. Donati, A. Li Bassi, C. S. Casari, and C. E. Bottani, Phys. Rev. B **79**, 045404 (2009).
[10] C. Wagner, R. Franke, and T. Fritz, Phys. Rev. B **75**, 235432 (2007).
[11] S. F. Alvarado, P. F. Seidler, D. G. Lidzey, and D. D. C. Bradley, Phys. Rev. Lett. **81**, 1082 (1998).
[12] M. Feng, J. Zhao, and H. Petek, Science **320**, 359 (2008).
[13] D. B. Dougherty, W. Jin, W. G. Cullen, G. Dutton, J. E. Reutt-Robey, and S. W. Robey, Phys. Rev. B **77**, 073414 (2008).
[14] J. Li, W.-D. Schneider, and R. Berndt, Phys. Rev. B **56**, 7656 (1997).
[15] L. Limot, J. Kröger, R. Berndt, A. Garcia-Lekue, and W. A. Hofer, Phys. Rev. Lett. **94**, 126102 (2005).
[16] J. G. Simmons, J. Appl. Phys. **34**, 1793 (1963).
[17] C. B. Duke, *Tunneling in Solids* (Academic, New York, 1969).
[18] R. J. Hamers, in *Scanning Probe Microscopy and Spectroscopy. Theory, Techniques and Applications*, edited by D. A. Bonnell (VCH, New York, 1993).
[19] X. Lu, M. Grobis, K. H. Khoo, S. G. Louie, and M. F. Crommie, Phys. Rev. B **70**, 115418 (2004).
[20] L. Limot, T. Maroutian, P. Johansson, and R. Berndt, Phys. Rev. Lett. **91**, 196801 (2003).
[21] J. Kröger, L. Limot, H. Jensen, R. Berndt, and P. Johansson, Phys. Rev. B **70**, 033401 (2004).
[22] J. Li, W.-D. Schneider, R. Berndt, O. R. Bryant, and S. Crampin, Phys. Rev. Lett. **81**, 4464 (1998).
[23] A. Schäfer, I. L. Shumay, M. Wiets, M. Weinelt, Th. Fauster, E. V. Chulkov, V. M. Silkin, and P. M. Echenique, Phys. Rev. B **61**, 13159 (2000).
[24] J. A. Stroscio and R. M. Feenstra, in *Scanning Tunneling Microscopy*, Methods of Experimental Physics Vol. 27, edited by J. A. Stroscio and W. J. Kaiser (Academic, New York, 1993).
[25] J. A. Stroscio, R. M. Feenstra, D. M. Newns, and A. P. Fein, J. Vac. Sci. Technol. A **6**, 499 (1988).

[26] Th. Berghaus, A. Brodde, H. Neddermeyer, and St. Tosch, Surf. Sci. **193**, 235 (1988).
[27] A. Sperl, J. Kröger, N. Néel, H. Jensen, R. Berndt, A. Franke, and E. Pehlke, Phys. Rev. B **77**, 085422 (2008).
[28] A. Sperl, J. Kröger, R. Berndt, A. Franke, and E. Pehlke, New J. Phys. **11**, 063020 (2009).
[29] G. Binnig, K. H. Frank, H. Fuchs, N. Garcia, B. Reihl, H. Rohrer, F. Salvan, and A. R. Williams, Phys. Rev. Lett. **55**, 991 (1985).
[30] R. S. Becker, J. A. Golovchenko, and B. S. Swartzentruber, Phys. Rev. Lett. **55**, 987 (1985).
[31] A. Franke and E. Pehlke (private communication). For calculations of constant-distance data the tip was placed 0.4–0.6 nm above the dimer and the distances between the maxima varied between 0.45 and 0.48 nm. The current was calculated in a Tersoff-Hamann approach (Ref. 3). The electronic structure of the silver dimer has been calculated using density functional methods described in Ref. 27.
[32] G. Hörmandinger, Phys. Rev. Lett. **73**, 910 (1994); Phys. Rev. B **49**, 13897 (1994).
[33] S. Crampin, J. Kröger, H. Jensen, and R. Berndt, Phys. Rev. Lett. **95**, 029701 (2005).
[34] J. Li, W.-D. Schneider, R. Berndt, and S. Crampin, Phys. Rev. Lett. **80**, 3332 (1998).
[35] J. Kliewer, R. Berndt, and S. Crampin, Phys. Rev. Lett. **85**, 4936 (2000).
[36] H. Jensen, J. Kröger, R. Berndt, and S. Crampin, Phys. Rev. B **71**, 155417 (2005).
[37] S. Crampin, H. Jensen, J. Kröger, L. Limot, and R. Berndt, Phys. Rev. B **72**, 035443 (2005).
[38] S. Å. Lindgren and L. Walldén, Phys. Rev. B **22**, 5967 (1980).
[39] H. P. Bonzel, Surf. Sci. Rep. **8**, 43 (1988).
[40] J. Kröger, D. Bruchmann, S. Lehwald, and H. Ibach, Surf. Sci. **449**, 227 (2000).